Evaluation of a 5 kWp photovoltaic hydrogen production and storage installation for a residential home in Switzerland

Hollmuller, Pierre; Joubert, Jean-Marc Eric; Lachal, Bernard Marie; Yvon, Klaus

How to cite

HOLLMULLER, Pierre et al. Evaluation of a 5 kWp photovoltaic hydrogen production and storage installation for a residential home in Switzerland. In: International journal of hydrogen energy, 2000, vol. 25, n° 2, p. 97–109. doi: 10.1016/S0360-3199(99)00015-4

This publication URL: https://archive-ouverte.unige.ch/unige:34585
Publication DOI: 10.1016/S0360-3199(99)00015-4

EVALUATION OF A 5 kW_p PHOTOVOLTAIC HYDROGEN PRODUCTION AND STORAGE INSTALLATION FOR A RESIDENTIAL HOME IN SWITZERLAND

Preprint (edited version in Int. Journal of Hydrogen Energy, 25, 2000, pp. 97-109)

Pierre HOLLMULLER, Jean-Marc JOUBERT[†], Bernard LACHAL and Klaus YVON*

Centre d'Etudes des Problèmes de l'Energie and Laboratoire de Cristallographie,

University of Geneva, Switzerland

e-mail : klaus.yvon@cryst.unige.ch

Abstract - The performance of a privately owned photovoltaic (PV) hydrogen production and storage installation in a one-family house at Zollbrück i. E. in Switzerland (altitude 630 m, latitude 46.9°N) has been studied. The manually controled system operates since 1991 and was built by its owner (M. Markus Friedli) mainly from commercial components. It consists of an array of roof mounted PV solar panels (65 m^2 surface, 5 kW_p average peak power, 8.4% average efficiency), a DC-DC converter (95% efficiency), an alkaline membrane electrolyzer (5 kW, 62% average electrolyzer efficiency), a hydrogen purification unit, a compressor, and two metal hydride storage tanks, a fixed one (capacity: 15 Nm^3) for in-house storage to operate houshold appliances running on hydrogen such as a stove and a laundry machine, and a mobile one (capacity 16 Nm^3) for running a hydrogen operated minibus. *In-situ* measurements during operation on 3 typical summer days and computer modeling based on standard meteorological data suggest a yearly hydrogen production of 1100 Nm^3 (16 Nm^3/m^2.year), corresponding to an average efficiency of 3.6% for converting solar energy into hydrogen fuel for seasonal energy storage.

[†])permanent address : LCMTR-CNRS, 1 Place A. Briand, F-92195 Meudon-Cedex, France

*)corresponding author

1. INTRODUCTION

Photovoltaic (PV) hydrogen is a renewable source of fuel and electricity [1]. Production plants are in operation in various countries such as Finland [2], Germany [3-6], Italy [7], Japan [8], Spain [9], Saudi Arabia [10], Switzerland [11] and US [12,13]. Most are demonstration units which are operated by public institutions (universities, national energy agencies), or built by utilities with a major involvent of public funds. Their principle aim is to investigate the technical and commercial feasability of seasonal storage of solar energy via hydrogen, and to provide educational training ground. Some installations also serve practical purposes such as the filling of ballons for meteorological studies in remote areas [11]. The power of the plants ranges between 150 Wp [12] and 266 kWp [3], and their location covers latitudes between 20°N [10] and 60°N [2]. The present report describes a private installation in Switzerland which has been built by its owner (M. Markus Friedli, CH-3436 Zollbrück i. E.) for domestic use without major support by public funds. The 5 kWp system consists mainly of commercial components and is operational since 1991. It is located in a region of moderate climate (altitude 630 m, latitude 46.9°N, average sunshine 1540 hrs/year, corresponding to 4020 MJ/m^2.year) and allows to produce and store hydrogen for both stationary (stove, laundry machine) and mobile applications (hydrogen powered car). The surplus PV electricity is either stored in a stock of lead acid batteries (1600Ah, 24V), or injected into the grid. It is manually operated and has so far not been used to maximize hydrogen production for seasonal energy storage. The aim of the present report is to describe this system (ch. 2), to evaluate its performance (ch. 3), to simulate its potential for seasonal energy storage (ch. 4), and to suggest possible improvements (ch. 5). No detailed cost estimates has been made on this installation so far. It is clear, however, that the installation as other systems of that type [3] can hardly compete at the moment with energy from fossil fuels (excluding externalities).

2. SYSTEM DESCRIPTION

The system is integrated into a one-family house shown in Fig. 1.

insert figure 1

The array of PV solar panels (see ch. 2.1) occupy a large area of the roof, while the control system and DC-DC converter (2.2), the electrolyzer (2.3), the hydrogen purification unit (2.4), the intermediate hydrogen storage tank and compressor (2.5), and the metal hydride storage tank for in-house hydrogen storage (2.6) are located in two cabinets of about $10m^2$ total surface which are situated at the first floor of the house. The minibus in the front of the house can be operated on hydrogen which is stored in a mobile metal hydride storage tank. A schematic diagram showing the various energy and materials flows of the system is represented in Fig.2.

insert figure 2

Solar radiation is transformed by PV panels into electric current which passes a control unit and a DC-DC transformer before being transformed by an electrolyzer into chemical energy (hydrogen) or stored in batteries and/or reinjected into the grid. A small part of auxilary energy is supplied by the electric grid for operation of the control unit, electrolyzer regulation, purification unit and hydrogen compressor. However, the electrolyzer can in principle also be operated from the public grid via an AC-DC converter. Water is needed both as a fuel and for cooling the electrolyzer and cleaning the hydrogen gas. The remaining thermal energy is evacuated by air. A small part of the hydrogen gas is used in the purification unit and

evacuated into air. The major part is transferred into an intermediate storage tank and then compressed for seasonal storage into a metal hydride storage tank. The latter is connected to house appliances such as a stove and a loundry machine (no longer in operation), and a second metal hydride storage tank in a minibus. The domestic grid is exclusively powered by the battery stack via a DC-AC converter and is completely separated from the public grid. The components shown in the left part of the diagram can be described as follows.

2.1 PV array

The PV array consists of 162 solar panels which are connected in series of 6 panels grouped into two modules. They cover a total surface of 65.2 m^2 (56.6 m^2 cell surface) and have a total nominal peak power of 7.4 kW_p (3.4 and 4 kW_p, for technical details see Table 1).

insert table 1

As shown in Fig. 3 the actually measured peak power during two sunny summer days is much lower (4.5 kW_p).

insert figure 3

This discrepancy is mainly due to

- an overestimation of the panel performance by the supplier ; the peak power as derived from U/I measurements and normalized for standard conditions, i.e. 1000 W/m^2 solar insulation and 25°C panel temperature, was found to be ~11% lower than the nominal power, and
- a loss of conversion efficiency due to the heating of the solar panels (up to 75°C at 1000 W/m^2 solar insulation).

A quadratic regression on the data for two days (see solid line in Fig. 3) yields a PV base efficiency of 8.9% which decreases at a rate of 0.2% per 100 W/m^2 solar insulation. A more global estimation of the seasonal efficiencies was made by using the PV simulation computer program PVSYST [14] and standard meteorological data available for that area. The values obtained vary between 9.7% (- 0.28% per 100W/m^2) for the summer season and 10.4% (- 0.23% per 100W/m^2) for the winter season (see Table 1). The estimated yearly average panel efficiency is 8.4% (see ch. 4).

2.2. Control unit and DC-DC converter

The unit consists of a regulator and a DC-DC converter which were developped and supplied by the Engineering School of Biel, Switzerland [15]. Their main purpose is to maximize the hydrogen production by matching the characteristics of the PV array and the electrolyzer (power point tracking), and to increase the charging efficiency of the lead acid batteries. Technical details are summarized in Table 2.

insert table 2

The system is manually operated and needs less than 30 W auxilliary power. Its average efficiency exceeds 95% at an incoming power greater than 1.8 kW. Various modes of operation are possible, such as hydrogen production from the two PV modules connected in parallel, charging the batteries from the PV modules and optional hydrogen production from the grid, charging the batteries from the 4 kW module and injection of electricity from the 3.4 kW module into the grid with optional hydrogen production from the grid, and hydrogen production from the 4 kW module with injection of electricity from the 3.4 kW module into the grid. The installation of the DC-DC converter and the suppression of the initially installed

DC-AC ondulator coupled to the AC-DC converter in the electrolyzer (ch. 2.3) decreased the losses by about 20 % [15].

2.3 *electrolyzer*

The commercial alcaline (KOH) type membrane model was originally designed for *continous* hydrogen production from the AC grid (for technical details see Table 3).

insert table 3

It had a maximum power of 10 kW and yielded about 2 Nm^3 hydrogen gas per hour at a pressure of 2 bar and a purity of 99.8%. For the present *intermittent* operation from PV power the original AC-DC rectifier in the electrolyzer was replaced by the DC-DC converter (ch. 2.2) and the operating power was limited to a lower threshold of 1.4 kW (1.8 kW at start-up) for reasons of safety, and to a upper threshold of 4.6 kW to minimize wear. These correspond to current limitations between 45 (55) A and 130 A, and a hydrogen production between 0.32 (0.40) and 0.95 Nm^3 per hour. The average electrolyzer efficiency as defined by the ratio of the lower heating value of hydrogen (LHV, 10 MJ/Nm^3) and the electric power used is 62 % (see ch. 4). Some 22 W electricity (from the grid) are needed for regulation, and up to 3 liter demineralized water per hour for electrolysis. At full operation the total water consumption is about 40 lit/hour, which includes about 30 lit/hour for cooling. Current *versus* tension characteristics at different operating temperatures were established by *ex-situ* measurements while bypassing the control unit so as to access low current densities as shown in Fig. 4.

insert figure 4

The solid line represents a fit to the 45°C data which is the average operating temperature of the electrolyzer. The data show the exponential rise of the cathodic and anodic overvoltages below 90 A, followed by a linear rise of the ohmic overvoltage, yielding an electrolyser voltage efficency which decreases with increasing current. The agreement between the *ex-situ* measurements and the *in-situ* measurements as performed in 5 minute steps and averaged over 3 days is satisfactory. The systematically higher voltage values at low current densities correspond to the start-up periods at the beginning of the day when the set-point temperature was not yet reached (see also Fig. 6).

2.4 *hydrogen purification*

The purification unit consists of a water bath, a condensor and a drying unit. The bath removes traces of the KOH electrolyte and uses water from the cooling circuit of the electrolyzer. The condensor is filled by a nobel metal which removes catalytically traces of oxygen. The drying unit consists of two molecular filters which remove water and are used in alternation. Originally designed to run under a constant hydrogen flow of 2 Nm^3/h, they are now controled by the electrolyzer regulation. They are capable of treating about 2 Nm^3 wet hydrogen gas each and have to be regenerated by heating under a hydrogen flux. This requires rather high amounts of both electric energy (200 W during 45 min for heating to 85°C, and 60 W in equilibrium, corresponding to about 0.13 kWh/Nm^3 hydrogen gas), and hydrogen gas (0.2 Nm^3/hour). The latter was estimated from the ratio between the purification outlet flow as measured from the pressure differential in the intermediate storage vessel and the purification inlet flow as calculated from the electrolyser characteristics, and found to represent an average loss of up to 8% of the total hydrogen generated by PV power. The

system runs on the grid and operates under a hydrogen pressure of about 2 bar (for technical details see Table 4).

insert table 4

2.5 *intermediate hydrogen storage tank and compressor*

The purified hydrogen gas is stored in an intermediate, cylindrically shaped steel vessel of about 450 liter capacity in the pressure range between 1.9 bar (upper setting to start the compressor charging the metal hydride tank) and 0.6 bar (lower setting to stop the compressor). The corresponding useful capacity of the vessel per compressor cycle is about 0.59 Nm^3 hydrogen gas. In order to meet the operating conditions of the metal-hydride storage tank (ch. 2.6) the gas is then compressed to about 29 bar by the compressor (for technical details see Table 5).

insert table 5

This requires a few minutes time and some 0.125 kWh grid power per compressor cycle (0.763 MJ/Nm^3, corresponding to 7.6% of the lower heating value of hydrogen). The estimated yearly average energy consumption is 810 MJ (see ch. 4).

2.6 *metal hydride storage tank*

The commercial unit [16] is situated at the floor of the electrolyzer control room and consists of a stack of metal cylinders which are filled with a hydrogen absorbing alloy (multisubstituted derivative of $TiMn_2$ [17]). They are embedded in a cooling circuit operating on tap water which allows to speed up thermalization during absorption (exothermic reaction)

and desorption (endothermic reaction). The circuit was switched on only for testing of the performance of the storage tank, but is not used during normal operation of the system. The total tank volume and weight is 91 lit and 235 kg, respectively, including 15 lit and 100 kg, respectively, of the alloy (for technical data see Table 6).

insert table 6

The storage characteristics of the metal hydride tank during asbsorption and desorption are shown in Fig. 5.

insert figure 5

The measurements were performed during the winter season by using the thermalizing circuit of circulating tap water at 5.3°C. The total reversible hydrogen capacity as measured between 1.2 and 27 bar was 15.2 Nm^3 (14 Nm^3 in alloy, 1.2 Nm^3 of compressed hydrogen in free volume). This quantity is similar to that of other metal hydride based PV hydrogen storage systems [6-9], but falls short by about 20% from the total capacity of 19 Nm^3 as stated by the supplier [16]. Likely reasons for this discrepancy are the difference between total and reversible storage capacity, aging, and the partial passivation of the metal hydride alloy due to contamination by impurities in the hydrogen gas during the past four years of operation. As expected, the failure to use the thermalizing circuit during normal operation reduced the actual storage capacity of the metal hydride tank further (see ch. 3). The heat production during a full hydrogenation cycle (14 Nm^3) was estimated based on the enthalpy of hydrogen absorption of -23 kJ/mole H_2, and found to be 14.4 MJ. The tank is connected to a hydrogen powered stove for cooking and a loundry machine (no longer in operation), and allows to charge a mobile metal hydride storage tank in a minibus (not decribed in this report) having

similar characteristics (16 Nm^3 capacity at room temperature and 40 bar pressure, 3 bar desorption pressure at -20°C)

3. DAILY PERFORMANCE

The performance of the system was evaluated by *in-situ* measurements during 3 summer days in 1996. Relevant data for one day (July 26) are presented in Fig. 6, which shows the evolution of the sunshine, hydrogen production, PV current and electrolyte temperature as a function of time.

insert figure 6

The weather conditions were sunny in the morning and cloudy in the afternoon. The measurements started at 8.00 a.m. The hydrogen production started at about 8.45 a.m. above the threshold setting of the electrolyzer of 55 A (~380 W/m^2 solar radiation), and increased continously as a function of time and insulation until noon. Note that the gross hydrogen production by the electrolyzer shown here was not actually measured, but calculated from the electrolyzer current, unlike the net hydrogen production after the purification unit (ch. 2.4). The electrolyzer temperature increased during about 1¼ hour until its stabilizing value of about 50°C was reached (10 a.m.). The first clouds appeared around 1 p.m. and lead to strong variations in the electrolyzer current, including a complete switch-off of the electrolyzer shortly before 5 p.m., followed by an almost immediate swich-on, until its definite switchoff around 5.30 p.m. The hydrogen gas was purified and stored in the intermediate storage vessel. Each time the pressure reached 1.9 bar, the compressor switched on and the hydrogen was transfered into the metal hydride storage tank. At the upper pressure limit of the latter, hydrogen was vented into air. Relevant data describing this procedure are shown in Fig. 7.

insert figure 7

The graphs show the temperature and pressure in the hydride storage tank, the compressor power and the rate of hydrogen venting as a function of time. During that day, the compressor swiched on 10 times, corresponding to a total hydrogen production of about 6 Nm^3. The temperature of the hydride bed increased from 15°C in the morning to 28°C at noon, while the pressure increased in intervals of about 1 hour stepwise from 10 to 30 bar, thus requiring a first venting of hydrogen at noon. A similar evolution was observed in the afternoon, requiring a second hydrogen venting in the evening. The total amount of vented hydrogen was 7.3 Nm^3 (including H_2 production from preceeding day), which is largely below the measured total capacity of the metal hydride tank (15 Nm^3). The failure to store the daily total production of hydrogen is due to the incomplete desorption of the metal hydride bed at the beginning of the measurements, and the inertia of heat transfer during absorption and desorption due to the neglect of using the thermalizing circuit during operation. A summary of the system performance on that day and a comparison with the performance on two other summer days is shown in Table 7.

insert table 7

4. SIMULATION OF YEARLY PRODUCTION POTENTIAL

The yearly hydrogen production potential was evaluated by computer modeling by using standard meteorological data and the measured efficencies of the various system components as described in ch. 2.1 - 2.5. In a first step, the dependencies of the PV power and hydrogen

production rate as a function of solar radiation were evaluated for a typical summer day as shown in Fig. 8.

insert figure 8

The graphs show a comparison between *in-situ* measurements as obtained in 5 minute steps during three summer days (data points) and fits to both the simulated PV power before (PVgross) and after (PVnet) the control unit, and the simulated hydrogen production rates before (H_2gross) and after (H_2net) the purification unit. The simulated gross PV power (thick broken line, top) is identical to the quadratic fit to the data shown in Fig. 3, whereas the simulated net PV power (thin broken line, top) is reduced by 4% due to the energy losses in the control unit (ch 2.2). The simulated gross hydrogen production rate (thick solid line bottom) was calculated from the electrolyser characteristics at 45°C as shown in Fig. 4, while the net hydrogen production rate (thin solid line, bottom) was reduced by 8% in order to take into account regeneration of the hydrogen purification unit (ch. 2.4). As expected, the fits compare well with the data of the *in-situ* measurements. The scattering of the latter is presumably a consequence of the inhomogenous exposure of the PV field to solar radiation due to the cloudy weather conditions, and the limited accuracy of the pressure differential method to measure the hydrogen production rate.

In a second step the yearly hydrogen production potential was evaluated by using standard meteorological data (temperature, incident solar energy) from a nearby meteorological station (Berne, distant at 25 km). The simulation of the gross PV power was performed in steps of one hour for a period of one year by using the computer program PVSYST [14] as a more precise alternative to the mean seasonal efficencies given in ch. 2.1, while the other variables (PVnet, H_2gross, H_2net) were calculated in the same manner as shown before. The auxilary

power needed from the grid was evaluated by adding the steady power requirements of the control unit (ch. 2.2) and the electrolyser (ch. 2.3), the variable ones of the purification unit during heating and at equilibrium (ch. 2.4), and the cyclic ones of the compressor (ch. 2.5). Results are summarized in Table 8.

insert table 8

From a yearly total incident energy of 293 GJ falling on 65 m^2 PV panels (i.e. 4020 MJ/m^2.year, corresponding to 1540 hours of sunshine with a direct incident radiation greater than $200W/m^2$) some 24.5 GJ of gross electric energy (23.4 GJ of net energy after the DC-DC transformer) are left for subsequent uses, corresponding to an average PV efficiency of 8.4%. Of these only 18.6 GJ are powerful enough to drive the electrolyzer, while the rest (4.9 GJ) are stored in batteries and/or or reinjected into the grid to compensate the auxiliary power (3 GJ) needed to operate the various components. From the 18.6 GJ used for water splitting some 1148 Nm^3 (11.5 GJ) hydrogen gas are obtained per year (average electrolyzer efficiency 62%), of which 1056 Nm^3 (10.6 GJ) are left after hydrogen purification and regeneration. This corresponds to an energy equivalence of about 300 liter fuel and a hydrogen production potential of about 16 Nm^3/m^2.year. The estimated percentage of PV power usable for energy storage *via* electrolytic hydrogen production and the various losses of the installation are shown in Fig. 9.

insert figure 9

The fraction of PV power stored in the form of chemical energy (hydrogen) is 43%, while the net storage in the batteries and/or injection into the grid amounts to 8% (light sections). The

total losses (dark sections) are 57%. They comprise 12% injected into the grid to compensate auxiliary energy use, 4% for DC-DC conversion, 29% for electrolysis and 4% for purification. Thus the early average efficiency of the system for converting solar energy into chemical energy for seasonal storage is 3.6% (0.43 x 0.084), which is about 30 times bigger than that of photosynthesis.

5. CONCLUSION

The performance of the present installation compares well with that of other PV hydrogen production plants [1-13]. Nervertheless, its hydrogen production and storage potential could be improved by the following measures :

1. Installation of an automatic control unit: allows operation of the installation in absence of house inhabitants and thus increases its efficiency.
2. Replacement of the hydrogen purification unit by one which does not consume hydrogen : allows to increases the net hydrogen production by about 8%.
3. Increase of the hydrogen storage capacity : the estimated amount for seasonal hydrogen storage (~ 200 Nm^3 hydrogen gas, assuming a uniform consumption over the year) requires a ten times bigger storage capacity. For reasons of safety and economics of operation, increasing the metal hydride reservoir is preferable over installing a stack of compressed gas cylinders, although it is more expensive. This underlines the need for developping new inexpensive and light weight hydrogen storage alloys.

Acknowledgements - This study has benefitted from valuable advise of Markus Friedli (Zollbrück), Maurice Maess (Belgium), Martin Aemmer (Interlaken) and André Mermoud (Geneva), and technical support by Jean-Luc Lorenzoni and Eric Pampaloni (Geneva).

REFERENCES

1. Ogden, J.M. and Nitsch, J. : Solar Hydrogen, ch. 22 in *Renewable Energy, sources for fuel and electricity* (eds. T.B. Johanssonnen, H. Kelly, A.K.N. Reddy, R.H. Williams), Island Press, Washington DC, 1993.

2. Kautranen, P.S., Lund, P.D and Vanhanen, J.P. : Development of a self-sufficient solar-hydrogen energy system. *Int. J. Hydrogen Energy*, 1994, **19**, 99-106 ; see also Vanhanen, J.P., Kautranen, P.S. and Lund, P.D. : Operating experiences of a phosphoric acid fuel cell in a solar hydrogen energy system. *Ibid*, 1997, **22**, 707-713.

3. Szyska, A. : Neunburg vorm Wald - test centre for solar hydrogen technology. *Int. J. Hydrogen Energy*, 1994, **19**, 823-841; see also Szyska, A. : Ten years of solar hydrogen demonstration project at Neunburg vorm Wald, Germany. *Ibid*, 1998, **23**, 849-860.

4. Steeb, H., Seeger, W., Aba Oud, H. : HYSOLAR : An overview on the German-Saudi Arabian programme on solar hydrogen. *Int. J. Hydrogen Energy*, 1994, **19**, 683-686.

5. Voss, K., Goetzberger, A., Bopp, G., Häberle, A., Heinzel, A., Lehmberg, H. : The self-sufficient solar house in Freiburg - results of 3 years of operation. *Solar Energy*, 1996, **58**, 17-23.

6. Barthels, H., Brocke, W.A., Bonhoff, K., Groehn, H.G., Heuts, G., Lennartz, M., Mai, H., Mergel, J., Schmid, L., Ritzenhoff, P. : Phoebus-Jülich : an Autonomous Energy Supply System Comprising Photovoltaics, Electrolytic Hydrogen, Fuel Cell. *Int. J. Hydrogen Energy*, 1998, **23**, 295-301.

7. Galli, S. and Stefanoni, M. : Development of a solar-hydrogen cycle in Italy. *Int. J. Hydrogen Energy*, 1997, **22**, 453-458.

8. Huang, Y.C, Goto, H., Sato, A., Hayashi, T., Uchida, H. : Solar energy storage by metal hydride. *Z. f. physik. Chem, N.F.*, 1989, **164**, 1391-1396.

9. Garcia-Conde, A.G. and Rosa, F. : Solar hydrogen production : a Spanish experience. *Int. J. Hydrogen Energy*, 1993, **18**, 995-1000.

10. Daous, M.A., Bashir, M.D. and El-Naggar, M.M. : Experiences with the safe operation of a 2kW solar hydrogen plant. *Int. J. Hydrogen Energy*, 1994, **19**, 441-445.

11. HYDROSOL : Production solaire d'hydrogène, ISM Payerne. NEFF project No 596 ; Zwischenbericht Mai 1995, NEFF, Pfluggässlein 2, CH-4001 Basel ; EWI AG, CH-8034 Zürich

12. Lehman, P.A., Chamberlin, C.E., Pauletto, G. and Rocheleau, M.A. : Operating experience with a photovoltaic-hydrogen energy system. *Int. J. Hydrogen Energy*, 1997, **22**, 465-470.

13. Hollenberg, J.W., Chen, E.N., Lakeram, K. and Modroukas, D. : Development of a photovoltaic energy conversion system with hydrogen energy storage. *Int. J. Hydrogen Energy*, 1995, **20**, 239-243.

14. PVSYST, logiciel pour systèmes photovoltaiques, A. Mermoud, GAP, Université de Genève, 1996

15. M. Aemmer and V. Crastan, *Solar-Wasserstoffanlage Friedli Zollbrück*, Ingenieurschule Biel, Fachgruppe für Energietechnik, Schlussbericht (EF-P+D(91)0112), 1993

16. Japan Metals & Chemicals Co., Ltd., 8-4 Nihombashi, Koami-cho, Chuo-ku, Tokyo 103, Japan.

17. Bernauer, O., Ziegler, K. : German patent DE 3,151.712 C1 (1981).

Table 1. Data of PV panels and array

panels

supplier	Siemens
model	Arcosolar M73 and M75
number of cells	33/panel
surface/panel	4.023 m^2 (total), 3.494 m^2 (net)
nominal power	M73 : 41 W, M75 : 48 W (at standard conditions : global solar radiation 1000W/m^2, cell temperature 25°C)
real power*	M73 : 37.8 W, M75 : 41.6 W
temperature	max. 75°C

array

connection	in series of 6, grouped in two modules	
module 1	42 M73, 48 M75	
module 2	72 M75	
total surface	65.2 m^2	
orientation	10°SSE azimutal, inclination 35°	
power	7.4 kW (nominal), 6.6 kW (real*), 4.5 - 5.0 kW (measured)	
efficiency	summer	9.7% - 0.28% per 100W/m^2 insulation**
	winter	10.4% - 0.23% per 100W/m^2 insulation**
	midseason	10.1% - 0.28% per 100W/m^2 insulation**
	yearly average 8.4%	

* as derived from U/I measurements normalized for standard conditions of 1000W/m^2 solar insulation and a panel temperature of 25°C, by using the program PVSYST[14].

** based on standard meteorological data and regression on input/output data in steps of one hour, as generated by PVSYST [14].

Table 2. Technical data of control unit and DC-DC converter [15]

supplier	Ecole d'ingénieurs de Bienne CH-2501 Bienne	
model	HMAX	
voltage (V)	entry	70 - 150 DC
	exit electrolyzer	28 - 38 DC
	exit batteries	22 - 28.5 DC
current (A)	entry	0 - 120 DC
	exit electrolyzer	30 - 300 DC
	exit batteries	0 - 300 DC
power (nominal)	11 kW (electrolyzer), 8.5 kW (batteries)	
auxiliary power	<30 W (950 MJ/year)	
dimensions	158x55x60 cm^3	
efficiency	96% at 1.8 kW entry and greater	

Table 3. Technical data of electrolyzer

supplier	VCST Hydrogen Systems (Belgium)	
model	IMET 2	
cell number	16	
cell surface	600 cm^2	
temperature	45°C (average), 50°C (setpoint)	
pressure	2 bar	
electrolyte	KOH (30 wt%, density 1.27 gcm^{-3})	
dimensions	0.60 x 0.80 x 1.79 m^3	
maximum power	9.5 kW (37 V, 250 A), 2Nm^3/h	
requirements		
water	electrolysis	3 lit/Nm^3
	cooling of H_2 gas	7.5 lit/hour
	cooling of cells	40 lit/Nm^3
regulation power	22 W (690 MJ/year)	
limitations for PV operation		
power	1400 W (1800 W at start-up) - 4600 W	
current	45 (55) A - 130 A	
hydrogen yield	0.32 (0.40) - 0.95 Nm^3/hour	
efficiency*	66 (65) - 60%, average 62%	

*ratio between the lower heating value of hydrogen and the electric power used

---

Table 4. Data of hydrogen purification units

dimensions	70 x 20 x 105 cm^3
temperature setting	85°C
start-up heating time	45 min (from 25 to 85°C)
heating power	60 W (200 W during start-up)
	estimated yearly average 510 MJ (0.13 kWh/Nm^3)
hydrogen requirement	0.2 m^3/hour
pressure	2 bar

Table 5. Data for intermediate hydrogen storage tank and compressor

storage tank	
supplier	Brand Anlagebau (CH)
volume	454(+/-13) liter
pressure	1.9 - 0.6 bar
hight	195 cm (total), 180 cm (vessel)
diameter	60 cm
H_2-capacity	0.59 Nm^3 (between 0.6 and 1.9 bar)
compressor	
supplier	Corken (USA)
model	D191 AM4FBAB
power	3.2 kW, estimated yearly average 810 MJ
time/cyle	150 s
power/cycle	0.125 kWh/0.59 Nm^3 (0.763 MJ/Nm^3)

Table 6. Data of metal hydride storage tank

supplier	Japan Metals & Chemicals [16]
pressure range	1.2 - 29 bar
capacity	19 Nm^3 (nominal at 20°C, 30 bar)
	15.2 Nm^3 (measured at 5.3°C, between 1.2 and 27 bar)
volume	91 lit (total), 15 lit (metal hydride)
weight	235 kg
alloy composition	$Ti_{0.98}Zr_{0.02}V_{0.43}Fe_{0.09}Cr_{0.05}Mn_{1.5}$ [17]
storage efficiency	1.8 wt% (alloy, total), 1.3 wt% (alloy, reversible)
	0.54 wt% (tank, reversible)
heat of absorption/desorption	14.4 MJ for 14 Nm^3

Tab. 7 : Daily performance on 3 consecutive summer days :

date	production period [hours]	insulation total [kWh/m^2]	insulation during H_2 production [kWh/m^2]	PVgross kWh	PVnet kWh	H_2gross Nm^3	H_2net Nm^3
26. 7. 96	8.8	6.6	6.1	*	27.8	6.2	5.9
27. 7. 96	3.4	3.3	1.6	7.2	6.4	1.5	1.4
28. 7. 96	5.2	3.9	3.0	13.1	11.4	2.7	2.5

*) measurement missing

Table 8. Annual hydrogen production potential

	energy GJ/year	MJ/m^2.year	hydrogen volume Nm^3/year	Nm^3/m^2.year
solar power				
solar radiation	292.7	4491	29134	447.1
PV gross (after panels)	24.5	393	2546	39.1
PV net (after DC-DC converter)				
to electrolyzer	18.6	286	1854	28.4
to batteries/grid	4.9	75	489	7.5
total	23.5	361	2343	35.9
hydrogen gross (after electrolyzer)	11.5	177	1148	17.6
hydrogen net (after purification)	10.6	163	1056	16.2
auxiliary power				
DC-DC transformer	0.95	15	95	1.45
electrolyzer	0.69	11	69	1.05
dryer	0.51	8	51	0.78
compressor	0.81	12	80	1.23
total	3.0	45	294	4.5

Figure captions

Fig. 1. House of M. Friedli in Zollbrück and hydrogen powered minivan ; courtesy of M. Friedli.

Fig. 2. Schematic diagram of the energy and materials flow.

Fig. 3. PV power *versus* insulation, as measured during 2 summer days in intervals of 5 min.

Fig 4. Electrolyser current *versus* tension at different temperatures (triangles and squares), data fit on the average operating temperature (solid line), and data from in-situ measurements over 3 days (crosses), in 5 minutes step.

Fig. 5. Storage characteristics of the metal hydride tank at 5.3 °C ; absorption from half filled to full tank (upper curve, right), total desorption (lower curve) and absorption from empty to half filled tank (upper curve, left).

Fig. 6. Solar radiation, hydrogen production, PV current and electrolyte temperature *versus* time on July 26, 1996.

Fig. 7. Temperature and pressure in metal hydride storage tank, compressor power and rate of hydrogen outlet *versus* time on July 26, 1996.

Fig. 8. PV power and hydrogen production rate *versus* solar radiation in collector plane during summer season: comparison between measurement (points) and simulation (solid lines).

Fig. 9. Estimated percentage of PV power usable for energy storage via electrolytic hydrogen production, and losses.

Fig. 1. House of M. Friedli in Zollbrück and hydrogen powered minivan (courtesy of Mr Friedli).

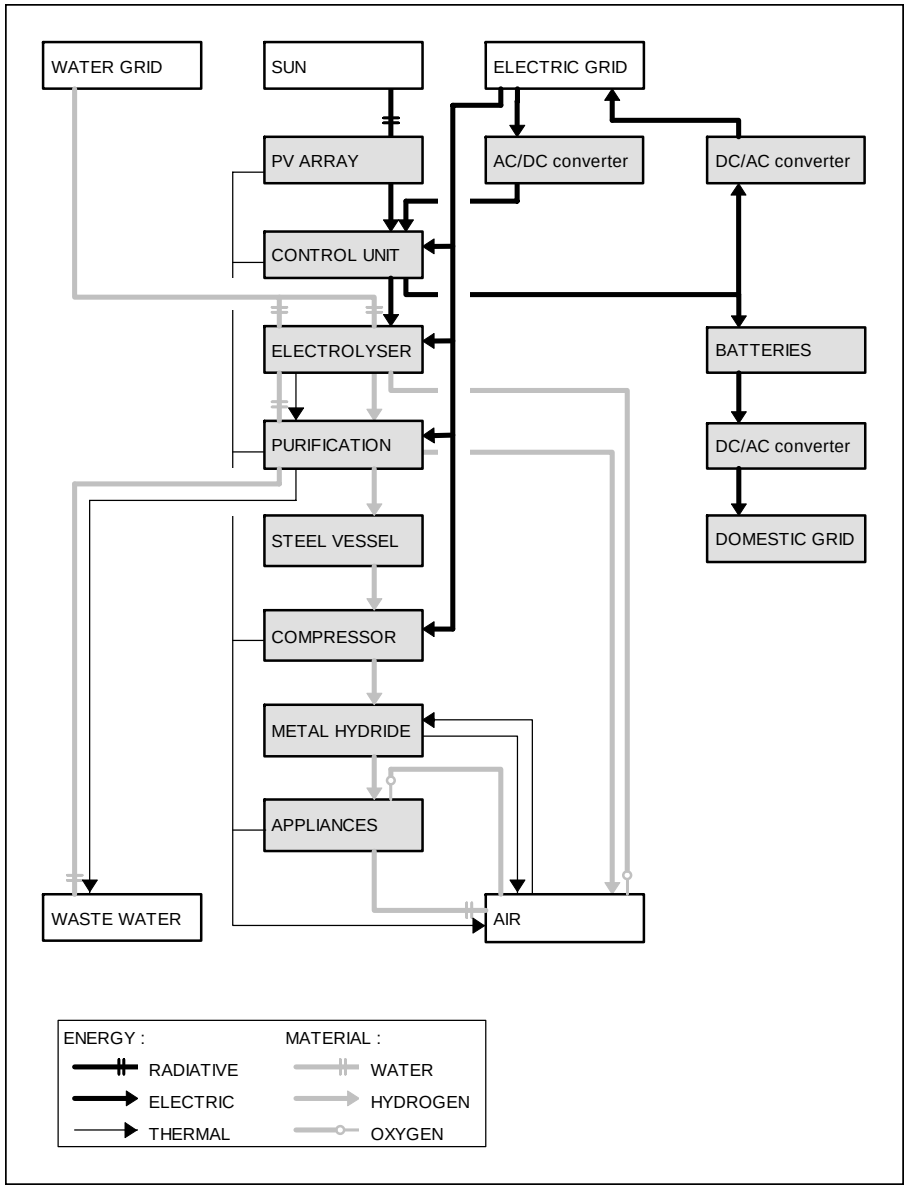

Fig. 2. Shematic diagram of the energy and material flow.

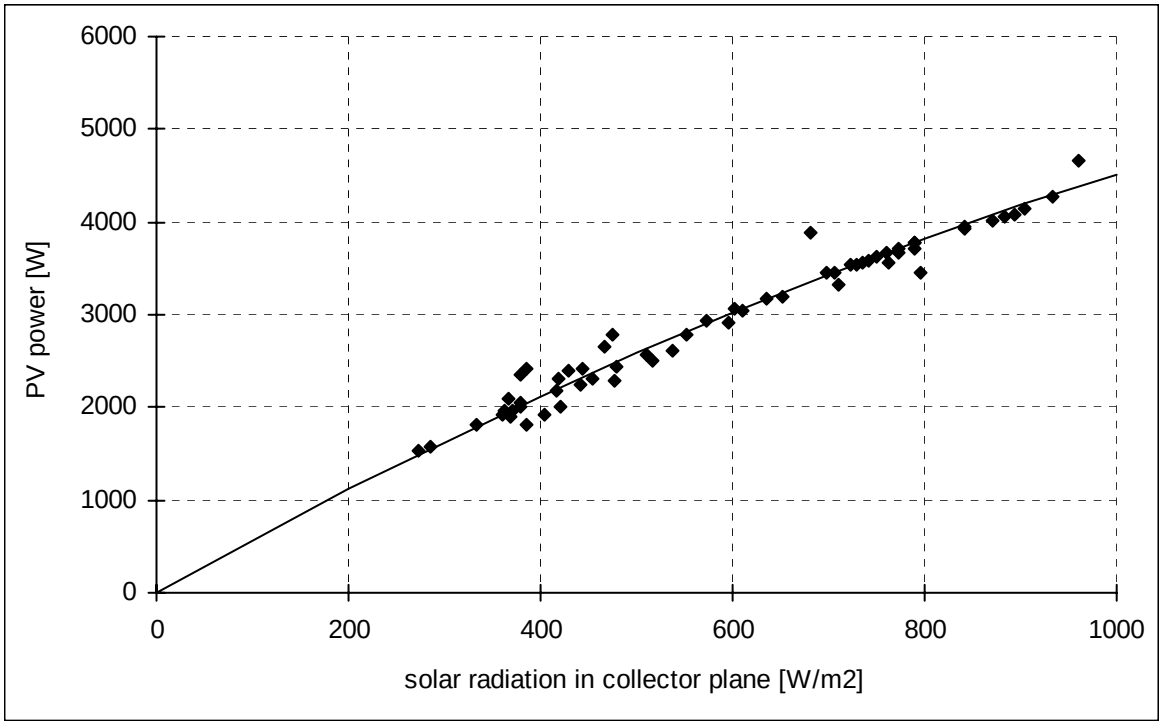

Fig. 3. PV power versus insulation, as measured during 2 summer days in intervals of 5 min.

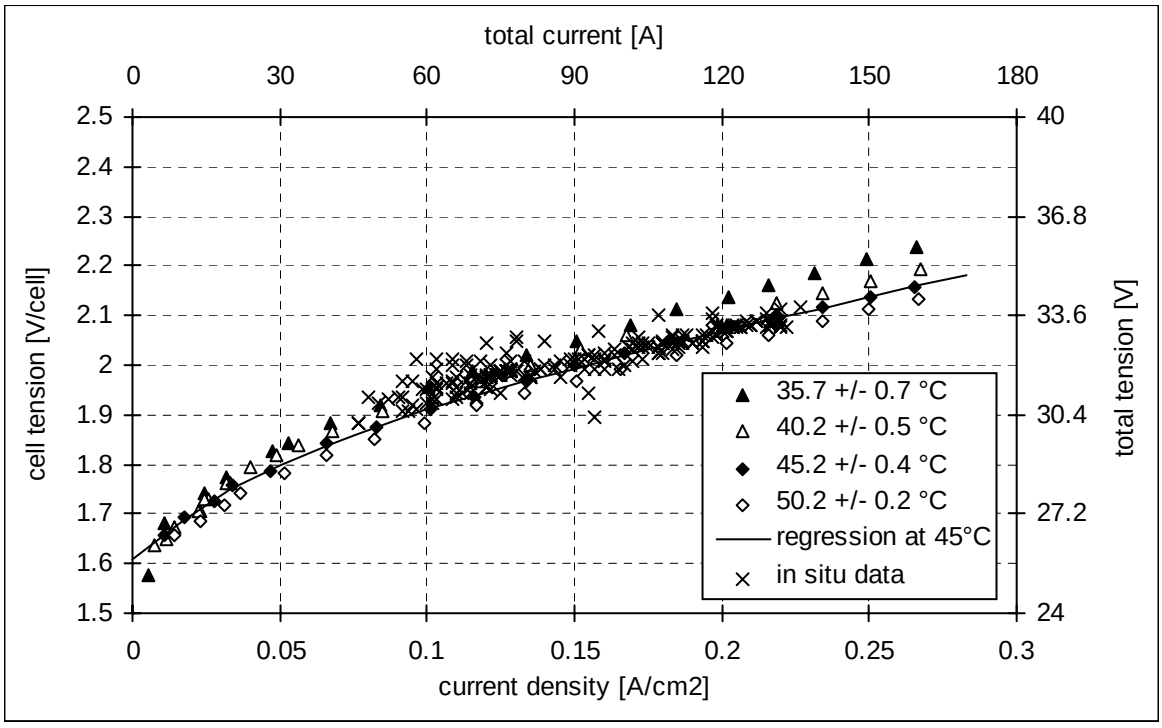

Fig. 4. Electrolyser current versus tension at different temperatures (triangles and squares), data fit on the average operating temperature (solid line), and data from in-situ measurements over 3 days (crosses), in 5 minutes step.

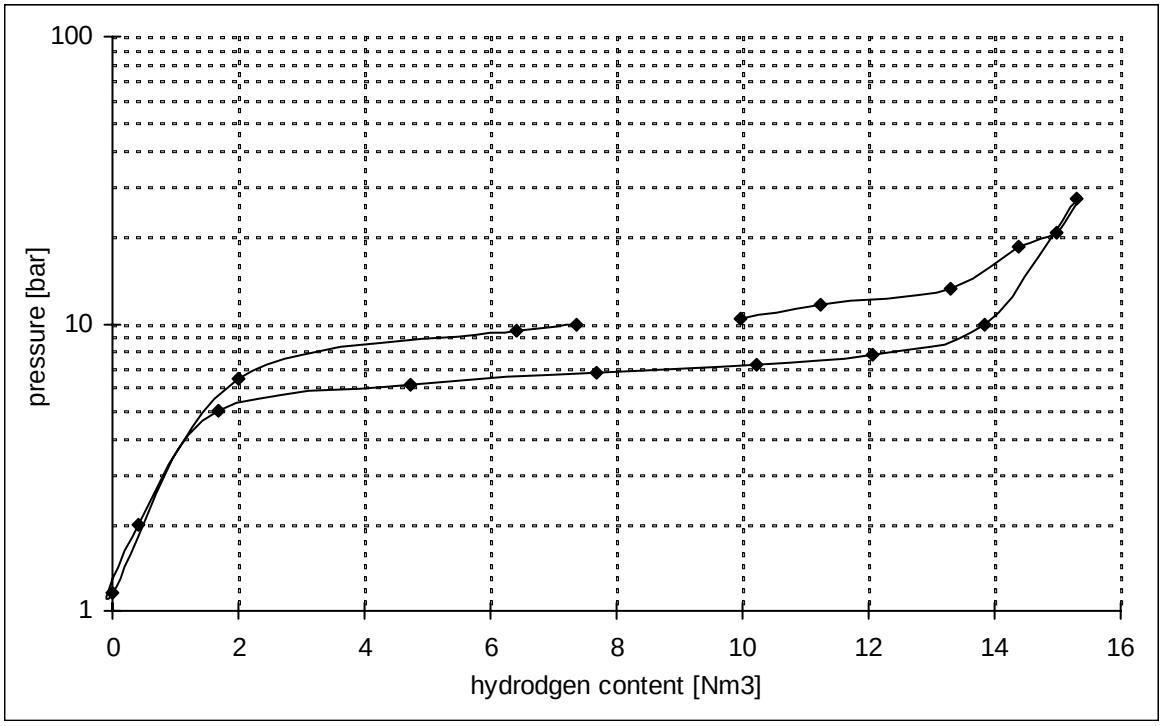

Fig. 5. Pressure-composition isotherms of the metal hydride tank at 5.3 °C during absorption (upper curve) and desorption (lower curve).

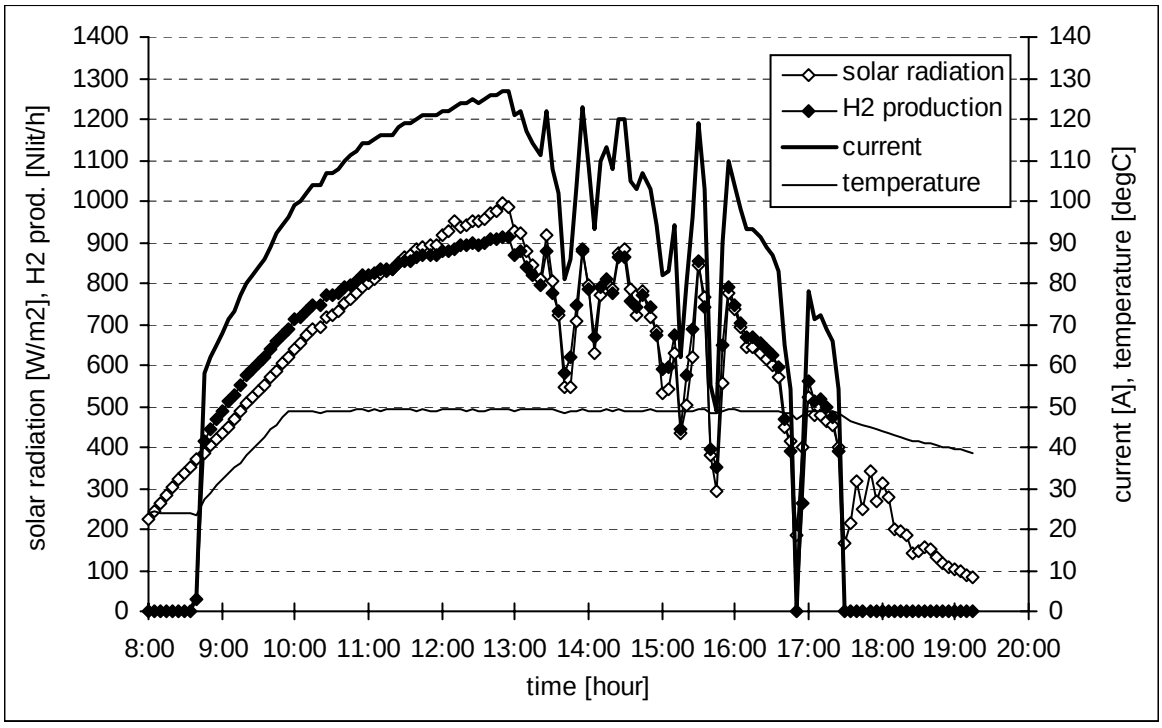

Fig. 6. Solar radiation, hydrogen production, PV current and electrolyte temperature versus time on July 26, 1996.

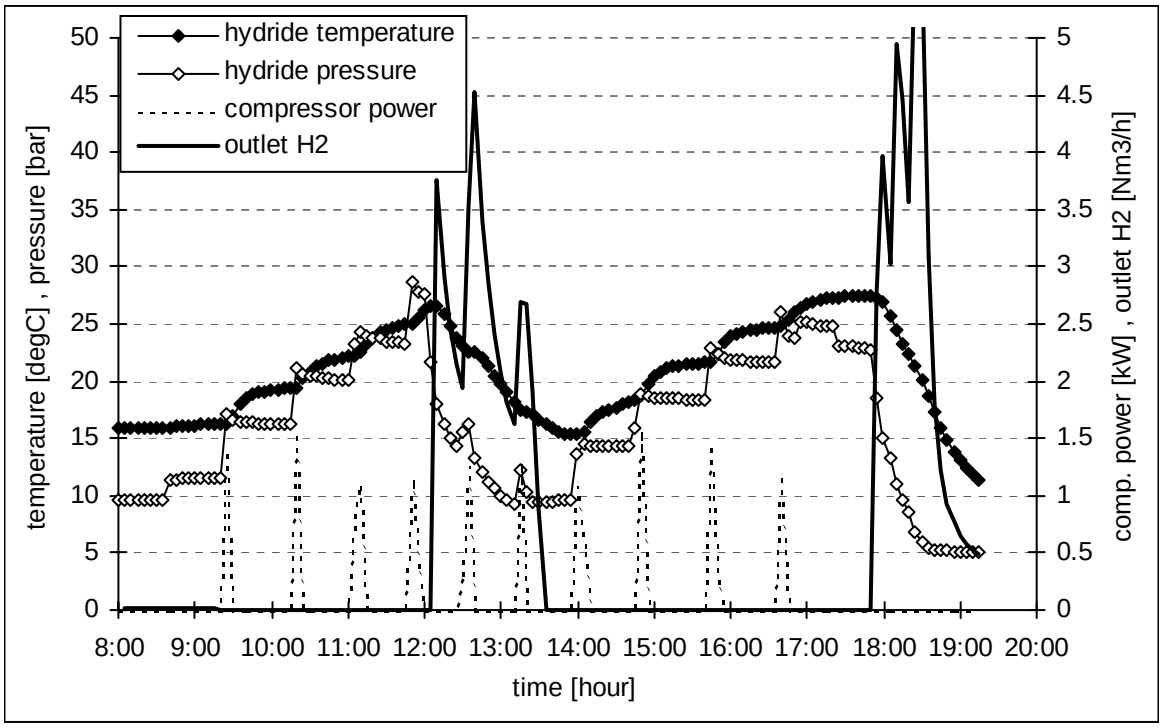

Fig. 7. Temperature and pressure in metal hydride tank, compressor power and rate of hydrogen outlet versus time on July 26, 1996.

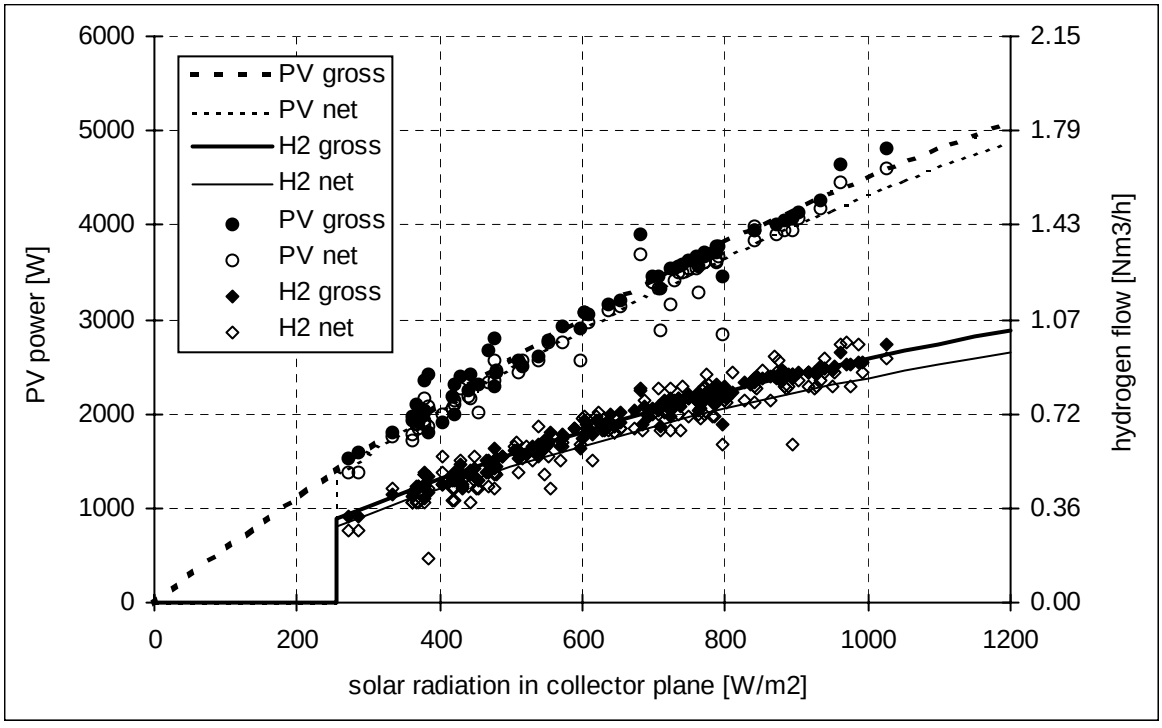

Fig.8. PV power and hydrogen production rate versus radiation in collector plane during the summer season : comparison between measurement (points) and simulation (solid lines).

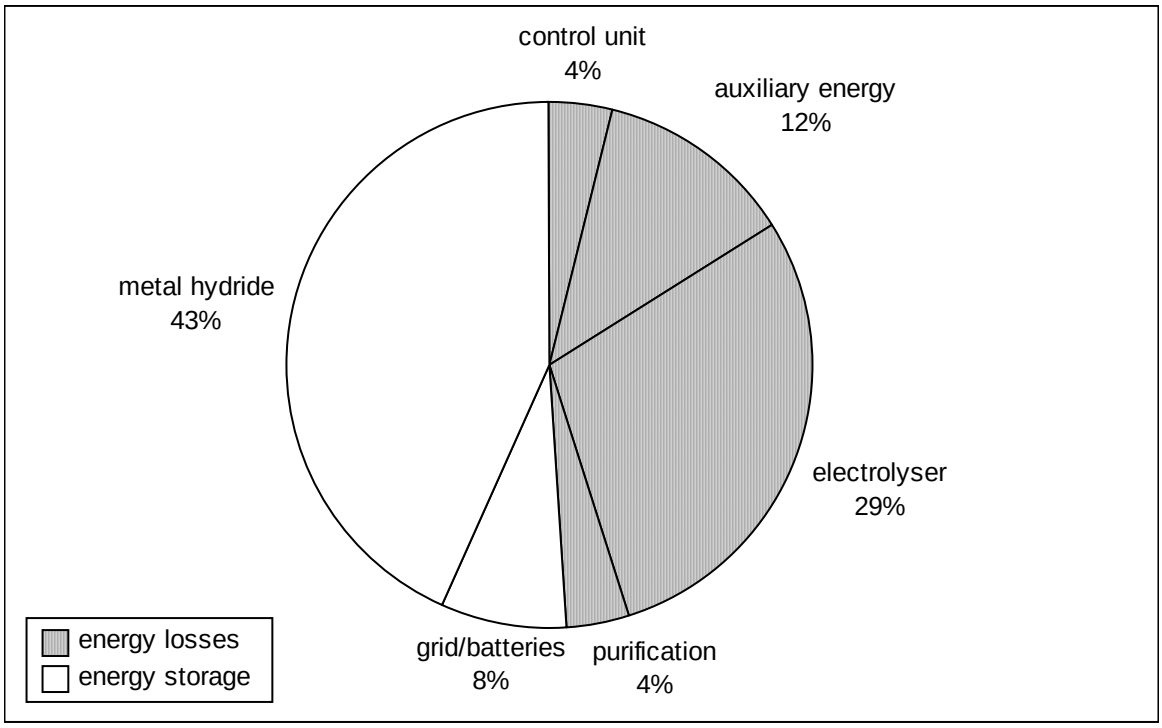

Fig. 9. Estimated percentage of PV power usable for energy storage via electrolytic hydrogen production, and losses.